

# Effect of MoSi<sub>2</sub> content on the lubricated sliding-wear resistance of ZrC–MoSi<sub>2</sub> composites

Beatriz Núñez-González<sup>a</sup>, Angel L. Ortiz<sup>a,\*</sup>, Fernando Guiberteau<sup>a</sup>, Nitin P. Padture<sup>b</sup>

<sup>a</sup> Departamento de Ingeniería Mecánica, Energética y de los Materiales, Universidad de Extremadura, 6071 Badajoz, Spain

<sup>b</sup> Department of Materials Science and Engineering, The Ohio State University, Columbus, OH 43210, USA

Received 30 July 2010; received in revised form 5 November 2010; accepted 21 November 2010

Available online 19 December 2010

## Abstract

The effect of MoSi<sub>2</sub> content (5, 10, and 20 vol.%) on the lubricated, sliding-wear behaviour of ZrC–MoSi<sub>2</sub> composites at room temperature is investigated and modeled. It was found that the resistance to sliding wear decreases markedly with increasing MoSi<sub>2</sub> content, with a greater rate of mild wear, an earlier transition from mild to severe wear, but essentially the same rate of severe wear. The analysis of the wear results using a mechanistic model indicated that the worsened sliding-wear resistance with the increase in MoSi<sub>2</sub> content derives from the decreased hardness and increased internal effective tensile stresses of the ZrC–MoSi<sub>2</sub> composite, which speed up the accumulation of damage induced by plastic deformation within the grains and shorten the onset of the grain-boundary fracture condition and subsequent grain pullout. Reduction of the MoSi<sub>2</sub> content thus emerges as an effective approach for making the ZrC–MoSi<sub>2</sub> composites more sliding-wear resistant under lubrication at room-temperature. These results may have important implications because ZrC holds promise for use in tribological applications requiring both wear resistance and electrical contact, and MoSi<sub>2</sub> is its commonest sintering additive.

© 2010 Elsevier Ltd. All rights reserved.

**Keywords:** ZrC; Sliding wear; Contact-mechanical properties; Tribology

## 1. Introduction

The favourable mechanical and thermal properties of ZrC make it one of the select group of compounds on the current short list of ceramic materials for extreme environments.<sup>1</sup> Not surprisingly, much of the current research on ZrC is focused on evaluating its use as a high-temperature aerospace material (leading edges, acreage thermal protection systems, scramjet flow-path components, rocket propulsion components, *etc.*). However, although they have been less explored, ZrC also possesses a unique combination of properties for tribological applications. In particular, it is not only harder (~25.5 GPa) and stiffer (elastic modulus ~392 MPa) than the common advanced ceramics (Al<sub>2</sub>O<sub>3</sub>, ZrO<sub>2</sub>, Si<sub>3</sub>N<sub>4</sub>, *etc.*), but is also more refractory (melting point ~3540 °C) and a better thermal conductor (~40 W m<sup>-1</sup> °C<sup>-1</sup>).<sup>2</sup> Thus, ZrC would alleviate and resist the frictional heating in sliding-contact appli-

cations better than other advanced ceramics, which make it particularly useful for the fabrication of a great variety of tribocomponents (bearings, wear parts, valves, seals, rollers, *etc.*). Another feature that distinguishes ZrC from the majority of common triboceramics is that its high electrical conductivity (~10<sup>6</sup> S m<sup>-1</sup>), similar to that of many metals, enables its use in tribological applications that require electrical contact, such as brushes, microelectromechanical devices, circuit breakers, motor vehicle starters, *etc.* In this context, ZrC could potentially provide electrical tribocomponents with the superior sliding-wear resistance not achievable today with metals, which cannot compete with ceramics in this important mechanical property.

Unlike other mechanical properties, the sliding wear of polycrystalline ceramics is controlled by average microstructural characteristics. This underscores the need to investigate the effects of microstructure on the sliding-wear resistance of ZrC if this is to be used for fabricating tribocomponents. One of these microstructural features is the vol.% of second phases because ZrC is intrinsically unsinterable in the pure state, and has to be densified with the help of additives. For this reason, in the present wear study we explore the role of the MoSi<sub>2</sub> content

\* Corresponding author. Tel.: +34 924289600x86726; fax: +34 924289601.

E-mail addresses: [alortiz@materiales.unex.es](mailto:alortiz@materiales.unex.es), [alortiz@unex.es](mailto:alortiz@unex.es) (A.L. Ortiz).

(5, 10, or 20 vol.%), doubtless the commonest sintering additive for ZrC. We find that reduction of the MoSi<sub>2</sub> content should be an effective approach to making ZrC–MoSi<sub>2</sub> composites more sliding-wear resistant under lubrication at room-temperature, and support this finding using a wear-mechanistic model.

## 2. Experimental procedure

Commercially available submicrometre powders of ZrC and MoSi<sub>2</sub> (in both cases Grade B of H.C. Starck, Berlin, Goslar, Germany) were used as starting materials. Three powder batches were prepared by combining the ZrC and MoSi<sub>2</sub> powders in relative concentrations of 95–5, 90–10, and 80–20 vol.%, respectively (abbreviated hereafter as ZrC–*x*%MoSi<sub>2</sub>, where *x* refers to MoSi<sub>2</sub> content in vol.%). The individual powder batches were attrition milled (01-HD, Union Process, Akron, OH, USA) for 3 h at 600 rpm using WC/Co balls (6.7 mm diameter) with a charge ratio of 24:1 to reduce particle size and promote intimate mixing of ZrC and MoSi<sub>2</sub>. The milled powders were hot-pressed (HP20-3560-20, Thermal Technology LLC, Santa Rosa, CA, USA) at 1900 °C for 1 h at 30 MPa pressure. The hot-pressing protocol was the same than used previously by others in ZrB<sub>2</sub>,<sup>3</sup> except for the final temperature and pressure. The surfaces of the hot-pressed samples were polished to a 1 μm finish and were characterized by scanning electron microscopy (SEM; S-3600N, Hitachi, Japan). Several micrographs of representative regions within the microstructures were recorded for grain size analysis, which was performed by an image analysis system using at least 300 grains for each ZrC–MoSi<sub>2</sub> composite.

Sliding-wear testing was performed at room-temperature using a multi-specimen tribometer (Falex, Faville-Le Vally Corp., Sugar Grove, IL) configured in the ball-on-three-disks geometry. In this testing configuration a commercial, bearing grade Si<sub>3</sub>N<sub>4</sub> ball (NBD 200, Cerbec, East Granby, CT) of radius 6.35 mm was rotated in contact with three flat disk specimens (thickness 2 mm, diameter 4 mm) aligned with their surface normals in tetrahedral coordination relative to the rotation axis and mounted onto a bearing assembly to ensure equal distribution of the applied load. Paraffin oil (Heavy Grade, Fisher Scientific, Fair Lawn, NJ) with a viscosity of  $\sim 3.4 \times 10^{-5}$  m<sup>2</sup>/s ( $\sim 34$  cst) at 40 °C was used as the lubricant to avoid any tribological effects such as friction-induced heating or triboreactions, and thus to study the vol.% MoSi<sub>2</sub> effect only. The contact load was 120 N and the rotation speed was 100 rpm, corresponding to a sliding velocity of  $\sim 0.04$  m/s. The wear tests were interrupted at intervals, and the diameters of the circular wear scars on each disk were measured under optical microscopy (two orthogonal measurements per disk, three disks per ZrC–MoSi<sub>2</sub> composite). After each interruption the specimens were put back in the tribometer in exactly the same position using a precision fixture. The wear-scar diameter was used to quantify the extent of wear damage. Finally, the wear damage was observed under SEM.

Conventional Vickers indentation tests (MV-1, Matsuzawa, Tokyo, Japan) were performed to evaluate the hardness and toughness of the ZrC–MoSi<sub>2</sub> composites. Tests were performed

with 98 N load, and the hardness and toughness values were determined using the standard procedure and formulas<sup>4,5</sup>; elastic modulus (*E*) values determined by the rule-of-mixture were used in the toughness calculations ( $E_{\text{ZrC}} = 392$  GPa,<sup>6</sup> and  $E_{\text{MoSi}_2} = 440$  GPa<sup>7</sup>).

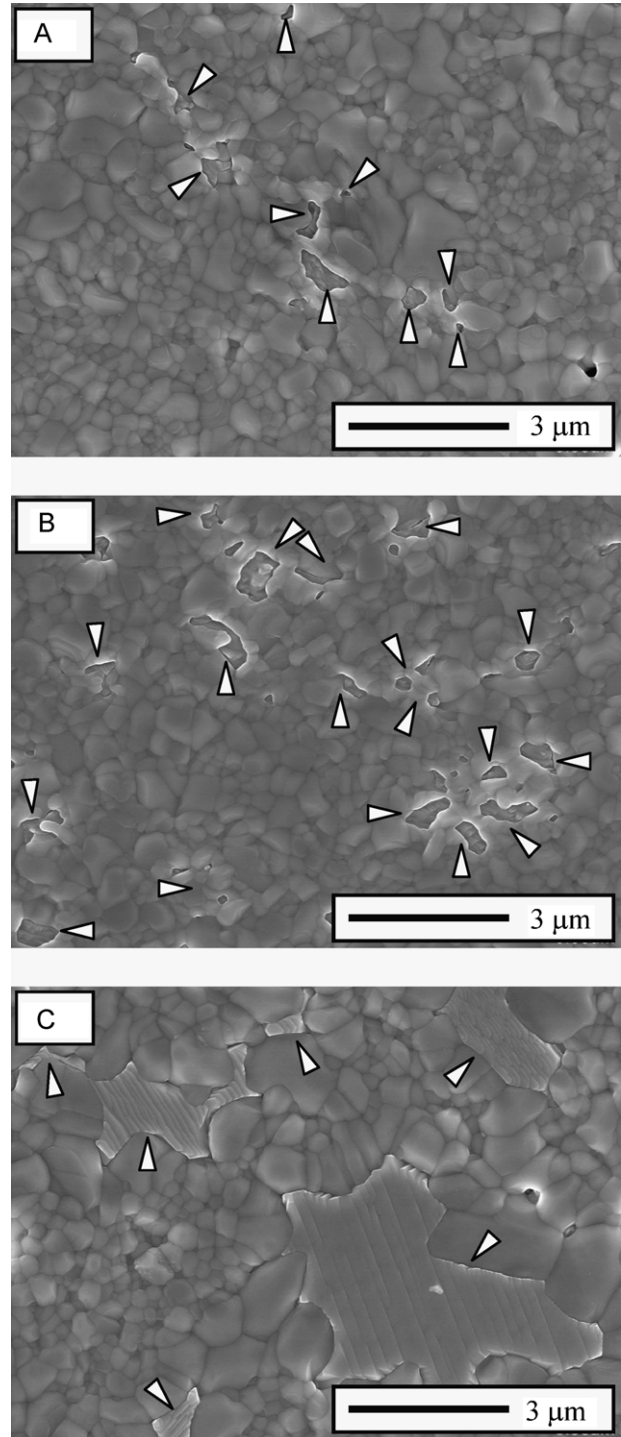


Fig. 1. SEM micrographs of the polished and thermally etched (1 h at 1500 °C in Ar) cross-sections of the ZrC–MoSi<sub>2</sub> composites prepared in this study: (A) ZrC–5%MoSi<sub>2</sub>, (B) ZrC–10%MoSi<sub>2</sub>, and (C) ZrC–20%MoSi<sub>2</sub>. The MoSi<sub>2</sub> phase is marked with arrows.

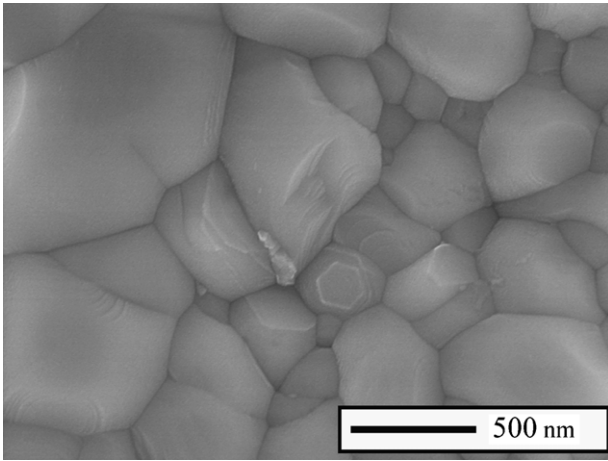


Fig. 2. SEM micrograph of the polished and thermally etched (1 h at 1500 °C in Ar) cross-sections of ZrC–5%MoSi<sub>2</sub> showing the grain size of the ZrC phase. The ZrC grain size is the same in ZrC–10%MoSi<sub>2</sub> and ZrC–20%MoSi<sub>2</sub>.

### 3. Results

Fig. 1a–c shows representative SEM images of the microstructure of the three ZrC–MoSi<sub>2</sub> composites. As can be seen in these micrographs, the three composites are dense and contain ZrC grains of the same size. These ZrC grains are very fine (less than  $0.5 \pm 0.2 \mu\text{m}$  in average) and have an equiaxed shape (see the SEM image of Fig. 2). Also evident in the micrographs of Fig. 1 is the increasing vol.% of MoSi<sub>2</sub> pockets in going from ZrC–5%MoSi<sub>2</sub> to ZrC–20%MoSi<sub>2</sub>. Table 1 lists the hardness and toughness measured by Vickers testing. It can be observed that with increasing MoSi<sub>2</sub> content in the composite the hardness decreases and the toughness increases. The decreasing hardness of the composite with increasing MoSi<sub>2</sub> content can only be attributed to the greater presence of the softer MoSi<sub>2</sub> phase ( $\sim 12 \text{ GPa}$ )<sup>8</sup> because the ZrC grains have the same size in the three composites and therefore the same hardness according to the Hall–Petch relationship.<sup>9,10</sup> The greater content of MoSi<sub>2</sub> is also responsible for the increasing toughness because the efficacy of the crack-wake bridging mechanism is known to increase with increasing thermal-expansion-mismatch stresses,<sup>11,12</sup> which in turns increase with increasing second-phase content.<sup>11,12</sup>

Fig. 3 shows the sliding-wear curves for the three ZrB<sub>2</sub>–MoSi<sub>2</sub> composites. One observes that these are of the same shape as the wear curves typical of other polycrystalline ceramics, *i.e.*, an initial section that corresponds to the mild wear regime, followed by an abrupt transition to a second section that corresponds to the severe wear regime.<sup>13</sup> It is also evident in

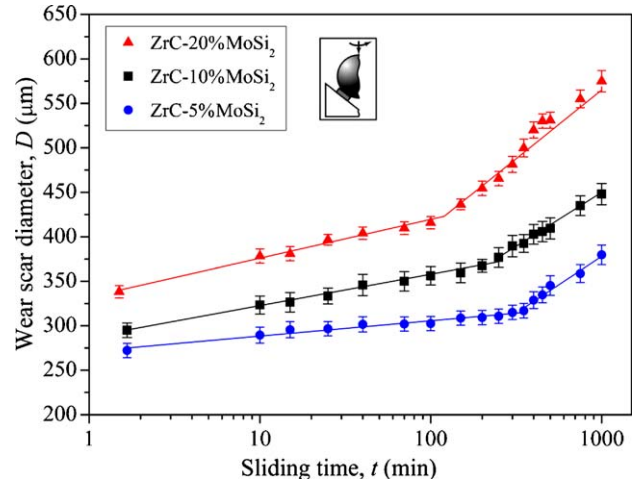


Fig. 3. Wear scar diameter as a function of the sliding time for the three ZrC–MoSi<sub>2</sub> composites prepared in this study. Each datum point represents the average of three specimens tested per ceramic; error bars represent data dispersion. The solid lines are fits to the data, with the discontinuities in the lines indicating mild wear to severe wear transitions. The inset is a schematic diagram showing a one-half cross-sectional view of the wear-testing geometry.

Fig. 3 that the wear curve of ZrC–5%MoSi<sub>2</sub> is below that of ZrC–10%MoSi<sub>2</sub>, which in turn is below that of ZrC–20%MoSi<sub>2</sub>. The rates of mild and severe wear calculated by fitting the empirical expression  $A + B \log t$  to the experimental data of  $D$  vs  $\log t$  in each regime are given in Table 1, together with the times of the wear-stage transition determined from the intersections of the fits to the mild and the severe wear regimes. As can be observed in Table 1, with increasing MoSi<sub>2</sub> content in the composite the rate of mild wear increases and the timing of the wear-stage transition is earlier, while the rate of severe wear is similar ( $\sim 10\%$  difference) for the three composites.

Fig. 4 is a low-magnification optical micrograph of the worn surface showing a typical wear scar. Fig. 5 shows representative SEM images of the damage within the wear scar in the three ZrB<sub>2</sub>–MoSi<sub>2</sub> composites at the end of the wear tests (1000 min). As expected in the fracture-controlled wear regime, in the three composites the damage is characterized by the presence of grooves within which there is evident grain pullout. Nevertheless, it is also clear in these micrographs that the severity of damage (*i.e.*, size of the grooves and the depth of the grain pullout) increases with increasing MoSi<sub>2</sub> content.

### 4. Discussion

The results presented above demonstrate that the lubricated sliding-wear resistance of the ZrC–MoSi<sub>2</sub> composites

Table 1  
Mechanical and sliding-wear properties of the three ZrC–MoSi<sub>2</sub> composites prepared in this study.

Sample	Vickers testing		Sliding-wear testing		
	Hardness (GPa; $\pm 0.1$ )	Toughness (MPa m <sup>0.5</sup> ; $\pm 0.1$ )	Mild-wear rate ( $\mu\text{m}/\log t$ )	Transition time (min)	Severe-wear rate ( $\mu\text{m}/\log t$ )
ZrC–5%MoSi <sub>2</sub>	22.8	2.6	$17 \pm 1$	350	$128 \pm 10$
ZrC–10%MoSi <sub>2</sub>	21.8	3.2	$34 \pm 1$	250	$117 \pm 6$
ZrC–20%MoSi <sub>2</sub>	20.7	3.6	$45 \pm 2$	120	$144 \pm 11$



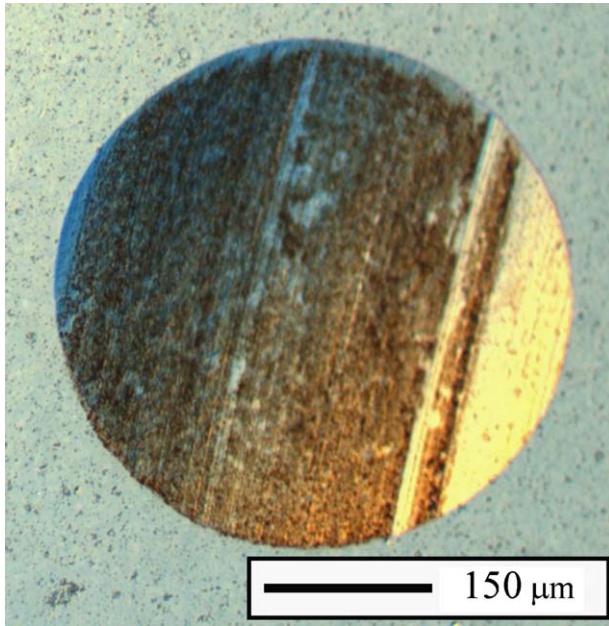


Fig. 4. Low-magnification optical micrograph of the worn surface of ZrC–10%MoSi<sub>2</sub> showing the circular wear scar after 1000 min of sliding.

decreases as the MoSi<sub>2</sub> content increases. To understand this behaviour, we invoke the governing sliding-wear theory in non-transforming polycrystalline ceramics with equiaxed-grain microstructures, which has been validated in previous studies.<sup>14–22</sup> It has been demonstrated that cumulative material removal during the sliding wear of ceramics occurs by two successive mechanisms—plastic deformation, followed by fracture. In the initial stages of sliding wear, plastic deformation damage in the form of dislocation pileups is introduced within the grains, inducing tensile stresses ( $\sigma_D(t)$ ) that bear up against the grain boundaries and accumulate as a function of sliding time  $t$ .<sup>14,16</sup> In the case of multi-phase ceramics, as are the ZrC–MoSi<sub>2</sub> composites, these stresses are added to the internal residual tensile stresses induced by the thermal expansion mismatch ( $q$ ), which are given by<sup>11,12</sup>

$$q \approx V(1 - V)E\Delta T\Delta\alpha \quad (1)$$

where  $V$  is the volume fraction of the second phase (*i.e.*, MoSi<sub>2</sub>),  $E$  the average elastic modulus,  $\Delta T$  the temperature range through which the composite is cooled without stress relaxation, and  $\Delta\alpha$  the thermal expansion mismatch. In this scenario, the time-dependent stress intensity factor ( $K(t)$ ) acting on the pre-existing grain-facet flaws under the wear contact can be written as<sup>14</sup>

$$K(t) = \psi(\sigma_D(t) + q)\beta\sqrt{d} \quad (2)$$

where the constants  $\psi$  and  $\beta$  are the crack geometry parameter and a scaling coefficient ( $\leq 1$ ), respectively, and  $d$  is the grain size. At a certain critical sliding time ( $t_c$ ) the stress intensity factor at grain-facet flaws will reach the grain-boundary toughness ( $K_{GB}$ )

$$K(t_c) = \psi(\sigma_D(t_c) + q)\beta\sqrt{d} = K_{GB} \quad (3)$$

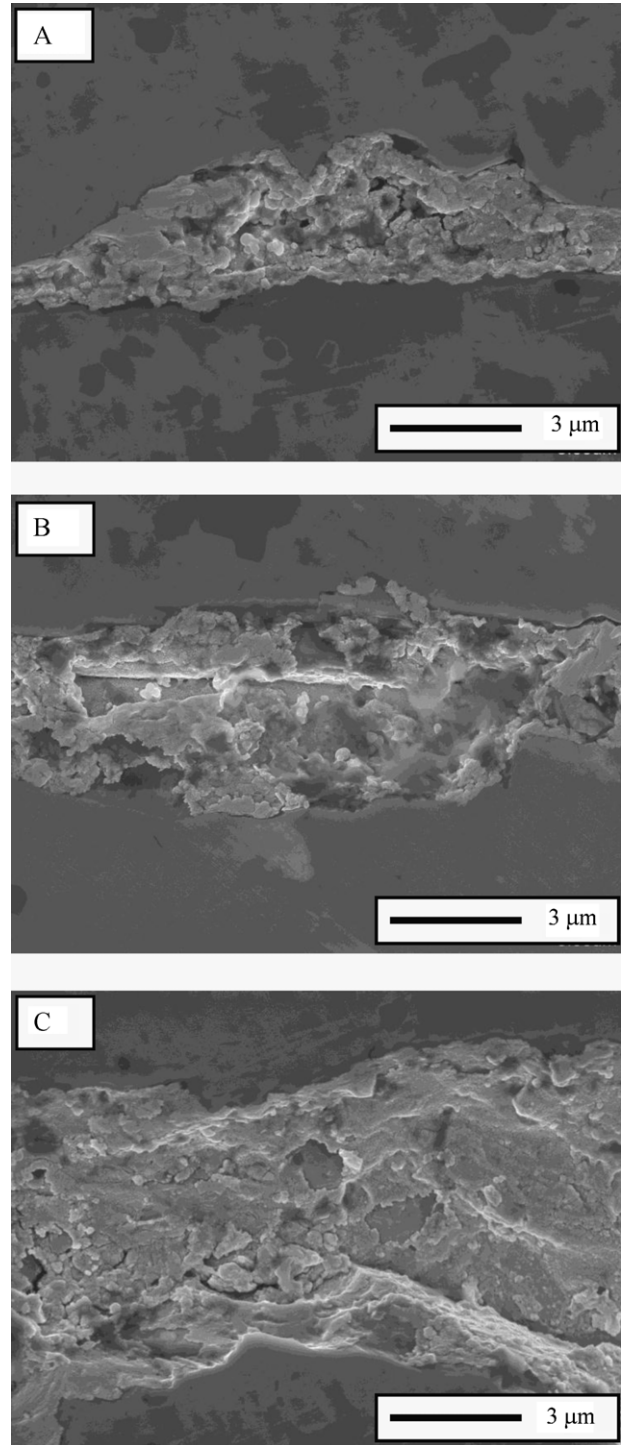


Fig. 5. SEM micrographs of the wear damage after 1000 min of sliding in: (A) ZrC–5%MoSi<sub>2</sub>, (B) ZrC–10%MoSi<sub>2</sub>, and (C) ZrC–20%MoSi<sub>2</sub>. Grain pullout in the images is indicative of the fracture-controlled wear regime.

and then grain-boundary fracture and subsequent grain pullout takes place representing the onset of the transition from mild deformation wear to severe fracture wear.

Let us apply this mechanistic model to explain the present wear data. It is evident from Eq. (2) that the size of the ZrC grains is not responsible for the differences in the wear behaviour because it is the same in the three composites. Hence, the

deterioration observed in the wear resistance of the ZrC–MoSi<sub>2</sub> composites as the MoSi<sub>2</sub> content increases is dictated only by the greater MoSi<sub>2</sub> content. According to the model, the increase in the MoSi<sub>2</sub> content should increase the rate of mild wear because this is controlled by the rate of accumulation of plasticity-induced stresses, and the hardness of the ZrC–MoSi<sub>2</sub> composites decreases with increasing MoSi<sub>2</sub> proportion. Furthermore, according to Eq. (2) the increase in MoSi<sub>2</sub> content also has a doubly detrimental effect which advances the onset of the grain-boundary fracture condition, *i.e.*, Eq. (3), and therefore shortens the time for the transition from mild to severe wear. First, there is an increase in the rate at which deformation-induced stress accumulates, which speeds up the rate of  $K(t)$  increase; and second, there is an increase in the effective tensile stress as predicted by the parabolic functional dependence  $q \propto V(1 - V)$  in Eq. (1).<sup>a</sup> It is not clear at this stage if the increase in MoSi<sub>2</sub> content affects the grain-boundary toughness, but if it does, it would be to make grain boundaries weaker, thus contributing to further shortening the time for the transition to the severe wear regime.<sup>20</sup> Finally, the increase in MoSi<sub>2</sub> content does not benefit the resistance to severe wear, despite the increase in toughness. In principle, tougher ceramics are expected to have lower rates of severe wear since this occurs by fracture and grain pullout. However, wear in this regime is a complex problem that also involves abrasion by the wear debris, and the abrasive-wear resistance is proportional to  $H_V^{1.425}/E^{0.8}$  so that softer ceramics with a greater elastic modulus abrade faster.<sup>13,23</sup> In addition, the amount of wear debris generated is greater in softer ceramics with earlier wear transitions because there is more grain pullout, so that the severity of the third-body abrasion is also greater. In consequence, unless the differences in toughness and hardness are large enough for one of these two mechanisms (fracture or abrasion) to clearly predominate, which is not the present case, the rate of severe wear is expected to be similar.

Based on these results and analyses, it emerges that the reduction of the MoSi<sub>2</sub> content should be an effective approach to making ZrC–MoSi<sub>2</sub> composites more sliding-wear resistant under lubrication conditions at room-temperature. Nevertheless, it should be noted that this strategy may not be applicable to unlubricated tribological situations involving effects such as friction-induced heating or tribo-reactions. This, however, remains to be elucidated by further tribological studies on ZrC–MoSi<sub>2</sub> composites.

## 5. Conclusions

We have investigated the dependence of the lubricated sliding-wear resistance of ZrC–MoSi<sub>2</sub> composites on their MoSi<sub>2</sub> content (5, 10, and 20 vol.%). It was observed exper-

imentally that the increase in MoSi<sub>2</sub> results in a pronounced worsening of the resistance of the ZrC–MoSi<sub>2</sub> composites to frictional sliding contact. The mechanistic analysis of the wear curves revealed that this is due both to the lower hardness which increases the rate of mild wear and shortens the onset of severe wear, and to the greater effective tensile stress which also contributes to shortening the time for the transition from mild to severe wear. The rate of severe wear is not affected by the MoSi<sub>2</sub> content because the greater toughness is compensated by the lower hardness and the greater severity of the third-body abrasion. Reduction of the MoSi<sub>2</sub> content thus emerges as a likely effective approach for making the ZrC–MoSi<sub>2</sub> composites more resistant to lubricated sliding wear at room-temperature. These results may have important implications because ZrC–MoSi<sub>2</sub> composites are attractive for use in engineering applications that require frictional sliding under electrical contact.

## Acknowledgements

This work was supported by the Ministerio de Ciencia y Tecnología (Government of Spain) and FEDER funds under Grant No. MAT 2007-61609.

## References

1. Wuchina E, Opila E, Opeka M, Fahrenholtz W, Talmy I. UHTCs: ultra-high temperature ceramic materials for extreme environment applications. *Electrochem Soc Interface* 2007;(Winter):30–6.
2. Shaffer PTB. Engineering properties of carbides. In: Schneider Jr SJ, editor. *Ceramics and glasses: engineered materials handbook*, vol. 4. Materials Park, OH: ASM International; 1991. p. 804–11.
3. Rezaie A, Fahrenholtz WG, Hilmas GE. Evolution of structure during the oxidation of zirconium diboride–silicon carbide in air up to 1500 °C. *J Eur Ceram Soc* 2007;**27**(6):2495–501.
4. Lawn BR. *Fracture of brittle solids*. 2nd ed. Cambridge, UK: Cambridge University Press; 1993.
5. Anstis GR, Chantikul P, Marshall DB, Lawn BR. A critical evaluation of indentation techniques for measuring fracture toughness: I. Direct crack measurements. *J Am Ceram Soc* 1981;**64**(9):533–8.
6. Landwehr SE, Hilmas GE, Fahrenholtz WG, Talmy IG, DiPietro SG. Microstructure and mechanical characterization of ZrC–Mo cermets produced by hot isostatic pressing. *Mater Sci Eng A* 2008;**497**(1–2):79–86.
7. Nakamura M, Matsumoto S, Hirano T. Elastic constants of MoSi<sub>2</sub> and WSi<sub>2</sub> single crystals. *J Mater Sci* 1990;**25**(7):3309–13.
8. Newman A, Jewett T, Sampath S, Berndt C, Herman H. Indentation response of molybdenum disilicide. *J Mater Res* 1998;**13**(9):2662–71.
9. Hall EO. The deformation and ageing of mild steel. 3. Discussion of results. *Proc Phys Soc London Sect B* 1951;**64**(381):747–53.
10. Petch NJ. The cleavage strength of polycrystals. *J Iron Steel Inst London* 1953;**174**(1):25–8.
11. Lawn BR, Padture NP, Braun LM, Bennison SJ. Model for toughness curves in two-phase ceramics: I. Basic fracture mechanics. *J Am Ceram Soc* 1993;**76**(9):2235–40.
12. Padture NP, Runyan JL, Bennison SJ, Braun LM, Lawn BR. Model for toughness curves in two-phase ceramics: II. Microstructural variables. *J Am Ceram Soc* 1993;**76**(9):2241–7.
13. Kato K, Adachi K. Wear mechanisms. In: Bhushan B, editor. *Modern tribology handbook*, vol. 1. FL: CRC Press; 2001. p. 273–300.
14. Cho S-J, Hockey BJ, Lawn BR, Bennison SJ. Grain-size and  $R$  curve effects in the abrasive wear of alumina. *J Am Ceram Soc* 1989;**72**(7):1249–52.
15. Cho S-J, Moon H, Hockey BJ, Hsu SM. The transition from mild to severe wear in alumina during sliding. *Acta Metall Mater* 1992;**40**(1):185–92.

<sup>a</sup> In particular, using the different volume fractions of MoSi<sub>2</sub> (*i.e.*, 0.05, 0.1, and 0.2) and taking  $\Delta\alpha \sim 1.8 \times 10^{-6} \text{ }^\circ\text{C}^{-1}$  for the thermal-expansion mismatch between ZrC ( $6.7 \times 10^{-6} \text{ }^\circ\text{C}^{-1}$ ) and MoSi<sub>2</sub> ( $(8 \text{ to } 9) \times 10^{-6} \text{ }^\circ\text{C}^{-1}$ ), the values of  $E$  calculated from the rule-of-mixture (*i.e.*, 394.4, 396.8, and 401.6 GPa), and  $\Delta T \sim 1875 \text{ }^\circ\text{C}$ , we calculated the internal residual tensile stresses to be 63, 120, and 217 MPa for ZrC–5%MoSi<sub>2</sub>, ZrC–10%MoSi<sub>2</sub>, and ZrC–20%MoSi<sub>2</sub>, respectively.

16. Cho S-J, Um C-D, Kim S-S. Wear and wear transition mechanism in silicon carbide ceramics during sliding. *J Am Ceram Soc* 1995;**78**(4):1076–8.
17. Wang Y, Hsu SM. Wear and wear transition mechanisms of ceramics. *Wear* 1996;**195**(1–2):112–22.
18. Cho S-J, Um C-D, Kim S-S. Wear and wear transition in silicon carbide ceramics during sliding. *J Am Ceram Soc* 1996;**79**(5):1247–51.
19. Thompson SC, Pandit A, Pature NP, Suresh S. Stepwise-graded Si<sub>3</sub>N<sub>4</sub>–SiC ceramics with Improved wear properties. *J Am Ceram Soc* 2002;**85**(8):2059–64.
20. Wang X, Pature NP, Tanaka H, Ortiz AL. Wear-resistant ultra-fine-grained ceramics. *Acta Mater* 2005;**53**(2):271–7.
21. Borrero-López O, Ortiz AL, Guiberteau F, Pature NP. Effect of microstructure on sliding-wear properties of liquid-phase-sintered  $\alpha$ -SiC. *J Am Ceram Soc* 2005;**88**(8):2159–63.
22. Borrero-López O, Ortiz AL, Guiberteau F, Pature NP. Microstructural design of sliding-wear-resistant liquid-phase-sintered sic: an overview. *J Eur Ceram Soc* 2007;**27**(11):3351–7.
23. Evans AG, Marshall DB. Wear mechanism in ceramics. In: Rigney DA, editor. *Fundamentals of friction and wear of materials*. American Society for Metals; 1981. p. 441–52.